Neurobiology of Aging 96 (2020) 148–154

Contents lists available at ScienceDirect

Neurobiology of Aging

journal homepage: www.elsevier.com/locate/neuaging

Brief communication

Cognitive enhancement, TAU phosphorylation reduction, and neuronal protection by the treatment of an LRRK2 inhibitor in a tauopathy mouse model

Sara Castro-Sánchez [b,c], Josefa Zaldivar-Diez [d], Enrique Luengo [e], Manuela G. López [e], Carmen Gil [a,d], Ana Martínez [a,d], Isabel Lastres-Becker [a,b,c,*]

[a] Centro de Investigación Biomédica en Red sobre Enfermedades Neurodegenerativas (CIBERNED), Madrid, Spain
[b] Instituto de Investigación Sanitaria La Paz (IdiPaz), Instituto de Investigaciones Biomédicas "Alberto Sols" UAM-CSIC, Madrid, Spain
[c] Department of Biochemistry, School of Medicine, Universidad Autonoma de Madrid, Madrid, Spain
[d] Centro de Investigaciones Biológicas-CSIC, Madrid, Spain
[e] Institute Teófilo Hernando for Drug Discovery, Department of Pharmacology, School of Medicine, Universidad Autónoma de Madrid, Madrid, Spain

ARTICLE INFO

Article history:
Received 25 February 2020
Received in revised form 7 July 2020
Accepted 1 September 2020
Available online 8 September 2020

Keywords:
TAU
Phospho-TAU
Neurodegeneration
Synaptic plasticity
Tauopathy
LRRK2

ABSTRACT

Leucine-rich repeat kinase 2 (LRRK2) is a protein kinase whose activity plays an important role in neurodegenerative diseases. Although mutations in LRRK2 gene are the most common cause of monogenic Parkinson's disease, it has been reported that LRRK2 may promote Tau phosphorylation, increasing its aggregation. Thus, the modulation of LRRK2 activity by small molecules able to inhibit this kinase activity could be an innovative therapeutic strategy for different tauopathies. We examined the therapeutic effects of a new benzothiazole-based LRRK2 inhibitor, known as JZ1.40, in a mouse model of tauopathy. Mice were injected in the right hippocampus with an adeno-associated vector expressing human-TAUP301L and treated daily with JZ1.40 (10 mg/kg, i.p) or vehicle for three weeks. JZ1.40 reaches the brain and modulates RAB10 and Tau phosphorylation at the epitopes modified by LRRK2. Moreover, JZ1.40 treatment ameliorates the cognitive impairment induced by TAUP301L overexpression, which correlates with prevention of granular cell layer degeneration by improving synaptic plasticity. These data show that JZ1.40 is neuroprotective in vivo, which is translated into cognition enhancement.

1. Introduction

Leucine-rich repeat kinase 2 (LRRK2) is a large multidomain protein kinase implicated in the regulation of several cellular pathways (Wallings et al., 2015). Mutations in LRRK2 are the most common cause of familial Parkinson's disease (PD), being G2019S mutation, which increases the activity of kinase LRRK2, the most prevalent one (Bailey et al., 2013; Ren et al., 2019). Moreover, postmortem brains of PD patients carrying LRRK2-G2019S within the kinase domain exhibited TAU phosphorylation and aggregation (Henderson et al., 2019; Ruffmann et al., 2012). Besides, LRRK2-G2019S has been also found in patients with certain tauopathies, such as progressive supranuclear palsy and corticobasal degeneration (Sanchez-Contreras et al., 2017; Vilas et al., 2018).

Regulation of TAU phosphorylation and the kinases implicated in these events are critical in tauopathies (Wang and Mandelkow, 2016). Recently, in vitro studies demonstrated that LRRK2 phosphorylates tubulin-associated, but not free TAU protein (Hamm et al., 2015; Kawakami et al., 2014). Moreover, LRRK2 mediates TAU phosphorylation at epitope Thr181 by direct interaction (Kawakami et al., 2014) while LRRK2 also activates other kinases enhancing their ability to target TAU such as AKT, members of the mitogen-activated protein kinase family and GSK-3β (Bailey et al., 2013). Furthermore, LRRK2 might modulate TAU phosphorylation by direct interaction with GSK-3β (Kawakami et al., 2014).

All these data suggest that the modulation of LRRK2 activity by small molecules able to inhibit this kinase activity could be an innovative therapeutic strategy not only for PD but also for tauopathies. We have recently described 2 chemical diverse new families of LRRK2 selective inhibitors (Salado et al., 2017; Zaldivar-Diez et al., 2019). Among them, the benzothiazole named as JZ1.40 is equipotent in LRRK2 and LRRK2-G2019S inhibition and predicted as brain permeable by parallel artificial membrane permeability assay methodology (Zaldivar-Diez et al., 2019). Therefore, in this work, we have studied the effects of JZ1.40 on the neurodegenerative process induced by overexpression of human TAU^{P301L} in a mouse model of

* Corresponding author at: Instituto de Investigaciones Biomédicas "Alberto Sols" UAM-CSIC, C/Arturo Duperier, 4, 28029 Madrid, Spain. Tel.: +34 915854449.
E-mail address: ilbecker@iib.uam.es (I. Lastres-Becker).

0197-4580/$ – see front matter
https://doi.org/10.1016/j.neurobiolaging.2020.09.006

tauopathy, as an exploratory study. We assessed the target engagement of JZ1.40 and evaluated the cognitive level of JZ1.40 treated mice in direct correlation with alterations in the synaptic plasticity in the hippocampus. Altogether, our data point to JZ1.40 as an interesting pharmacological probe to assess the role of LRRK2 inhibition in tauopathies.

2. Materials and methods

2.1. Animals and treatment

Each experimental group consisted of n = 14 male wild-type (WT) C57BL/6 mice of 6 months of age (see time-line diagram). The mice were bred and housed (3-4 mice per cage) in temperature-controlled cages (~23 °C) under a 12/12 hours light/dark cycle with free access to water and standard chow in the Autonomous University of Madrid Animal Core. Viral vector injections were performed under ketamine/xylazine anesthesia (8 mg/kg ketamine and 1.2 mg/kg xylazine) on adult mice. Surgery was performed using a stereotaxic frame (Stoelting, Wood Dale, IL). In total, 2 μL viral suspension containing 10E8 TAUof recombinant adeno-associated virus (AAV) vectors of serotype 6, which express mutant $hTAU^{P301L}$ under control of the human synapsin 1 gene promoter, was injected in the right hippocampus (ipsilateral side) as described before (Castro-Sánchez et al., 2019; Cuadrado et al., 2018; Lastres-Becker et al., 2014) left hemisphere of the brain was used as a control (contralateral side). Stereotaxic coordinates: −1.94 mm posterior, −1.4 mm lateral, and −1.8 mm ventral relative to bregma. Based on in vitro and cellular potency, a dose of 10 mg/kg i.p. was selected for JZ1.40 treatment. This compound or vehicle was given daily for 3 weeks. All experiments were performed in a P2 biosafety facility by certified researchers according to regional, national, and European regulations concerning animal welfare and animal experimentation and were authorized by the Ethics Committee for Research of the Autonomous University of Madrid with PROEX 279/14. Every effort was taken to minimize the number of animals used and their suffering. After surgery, the animals were kept under constant attention, in case they had symptoms of suffering, and in that case, they were sacrificed. The total number of mice used in the whole study was 35 (n = 14 WT-vehicle (VEH); n = 14 WT-JZ1.40 [3 animals died 24–48 hours after surgery] having n = 11 for final analysis; n = 7 WT mice as a control for novel object recognition [NOR] test). No sample calculation was performed. n = 9 WT-VEH and n = 7 WT-JZ1.40 animals that were used to dissect the brain and biochemical analysis (n = 5 WT-VEH and n = 4 WT-JZ1.40 samples for RNA checking; n = 4 WT-VEH and n = 3 WT-JZ1.40 samples for sarkosyl solubility analysis) were sacrificed by cervical dislocation. n = 5 WT-VEH and n = 4 WT-JZ1.40 animals that were used to fix the brain and make coronal cuts were given intracardiac perfusion with saline and subsequently 4% paraformaldehyde. To confirm the proper stereotaxic delivery, 30-μm thick sections from the hippocampus were stained with an antibody that specifically recognizes human TAU protein. Animals without proper expression of TAU were excluded (data not shown).

2.2. Randomization and blinding

Animals were randomized for treatment. Data collection and evaluation of all experiments were performed blindly of the group identity. The data and statistical analysis were performed with the recommendations on experimental design and analysis in pharmacology (Curtis et al., 2018).

2.3. Behavioral test

The NOR test was used to assess recognition memory and was performed as described (Leger et al., 2013). The amount of time spent exploring the novel (TN) or familiar (TF) object was recorded and the differences were represented as Discrimination Index (DI). DI allows discrimination between the novel and familiar objects: [DI = (TN − TF)/(TN + TF)].

2.4. Protein fractions of mouse kidney and brain cortex tissues

Protein lysates from mouse kidney and brain cortex tissues were homogenized in RIPA buffer (25 mM Tris-HCl pH 7.6, 150 mM NaCl, 1 mM ethylene glycol-bis(β-aminoethyl ether)-*N*,*N*,*N*′,*N*′-tetraacetic acid, 1% NP-40, 1% sodium deoxycholate, 0.1% SDS, 1 mM phenylmethylsulfonyl fluoride, 1 mM Na_3VO_4, 1 mM NaF, 1 μg/mL leupeptin). Homogenates were centrifuged at 15,900 *g* for 15 minutes at 4 °C. Protein concentration was determined by Pierce bicinchonic acid protein assay (Thermo Scientific) and 50 μg of protein was loaded for immunoblotting.

2.5. Sarkosyl-soluble and -insoluble fractions of mouse hippocampi

Ipsilateral hippocampi were homogenized in buffer A (0.1 M buffer MES pH 7, 1 mM EDTA, 0.5 mM $MgSO_4$, 1 M sucrose, 1 mM NaF, 1 mM Na_3VO_4, 10 μg/mL leupeptin and phenylmethylsulfonyl fluoride). Homogenates were centrifuged at 108,600 *g* for 20 minutes at 4 °C. To obtain the sarkosyl-insoluble fraction, the pellets were resuspended in RAB buffer described in Ren and Sahara (2013), vortexed for 1 minute at room temperature, incubated at 4 °C overnight, and then centrifuged at 374,670 *g* for 30 minutes at 4 °C. The supernatants were collected as sarkosyl-soluble fractions, and the pellets, sarkosyl-insoluble fractions, were resuspended in RAB buffer.

2.6. Immunoblotting

Sarkosyl-insoluble and -soluble fractions, as well as protein extracts from mouse kidney and brain cortex were resolved in sodium dodecyl sulfate-polyacrylamide gel electrophoresis and transferred to Immobilon-P membranes (Millipore). These membranes were analyzed by using the primary antibodies given in Supplementary Table 1, and appropriate peroxidase-conjugated secondary antibodies. Proteins were detected by enhanced chemiluminescence.

2.7. Immunofluorescence on mouse tissue and quantification of the dentate gyrus area

The protocol followed was previously described (Castro-Sanchez et al., 2018). Primary and secondary antibodies are described in Supplementary Table 1. The area of the dentate gyrus (contralateral vs. ipsilateral) from mice treated with vehicle or JZ1.40 stained with DAPI (4',6-diamidino-2-phenylindole) or anti-calbindin D28K was analyzed by Image J program. A total of 6 images per side and condition was analyzed as follows. The images are transformed into 16 bits with the Image J program. Then, with the “Free Hand Selection” tool of the Image J program, we manually selected only the dentate gyrus area of each image stained with DAPI or anti-calbindin D28K. The dimension of the dentate gyrus inside the selected area was quantified using the “Measure” tool in Image J program and the raw results measured in inches were represented.

2.8. Data and statistical analysis

Data are presented as mean ± standard error of mean. To determine the statistical test to be used, we employed GraphPad InStat 3, which included the analysis of the data to normal distribution via Kolmogorov-Smirnov test. Also, statistical assessments of differences between groups were analyzed (GraphPad Prism 6, San Diego, CA) by unpaired Student's *t*-tests when normal distribution and equal variances were fulfilled, or by the non-parametric Mann-Whitney test. One and two-way analysis of variance with post hoc Bonferroni test was used, when the *F* statistic was significant. $p < 0.05$ was considered statistically significant. At least 3 independent experiments were performed in duplicate with all the assays.

3. Results

3.1. Target engagement of JZ1.40

In order to confirm that JZ1.40 could modulate LRRK2 kinase activity, we performed target engagement experiments in different tissues of treated animals such as the brain (cortex) and peripheral tissue (kidney) where LRRK2 is abundantly expressed. Recent experiments show that a possible way of measuring LRRK2 activity and thus LRRK2 inhibitor engagement is by measuring its downstream substrate, the phosphorylation of RAB10 (Eyers, 2016; Ito et al., 2016). We quantified the amount of phosphorylated RAB10 at Thr73 both in the kidney and brain. Data analysis indicates that JZ1.40 treatment significantly decreases the levels of phospho-RAB10 in the kidney (n = 8 per group) (Fig. 1A) and also in the brain cortex (n = 9 per group) (Fig. 1B). These results demonstrate that JZ1.40 inhibits LRRK2 activity in vivo, and is able to cross the blood-brain barrier.

3.2. LRRK2 inhibition in vivo modulates TAU hyperphosphorylation and increases p-TAU solubility

Next, we analyzed whether the LRRK2 inhibitor could modulate TAU phosphorylation in vivo through 2 different approaches. First, we determined if JZ1.40 can modulate insoluble TAU aggregates in the brain using sarkosyl extraction as a standard protocol (Ren and Sahara, 2013). There is a consensus that sarkosyl-insoluble TAU correlates with the pathological features of tauopathy. Ipsilateral hippocampi of animals treated with vehicle showed an increase in hyperphosphorylated TAU at Thr181 in the sarkosyl-insoluble fraction (SI) in comparison to the hippocampi of JZ1.40 treated animals indicating that p-TAU accumulates in the hippocampus (Fig. 1D). But when we analyze the levels of total TAU, we observed that the treatment with JZ1.40 decreases the levels of TAU in such a way that when we normalize the levels of p-TAU versus total TAU, it seems that there are no changes between groups (Fig. 1D). However, regarding the soluble fraction SS, we observed that the treatment with JZ1.40 increases the phosphorylation of TAU compared to the hippocampi treated with VEH (Fig. 1C). Furthermore, we again observe that the inhibitor JZ1.40 decreases the total levels of TAU again, in such a way that in the normalization of p-TAU versus total TAU this phosphorylation is further enhanced. Our data seem to indicate that the LRRK2 inhibitor JZ1.40 modulates TAU levels by increasing in the soluble fraction (SS), and indicating a reduction of p-TAU in the aggregates. These results were confirmed using the AT8 antibody, which recognized phosphorylation of TAU at Ser202/Thr205 (Fig. 1C and D). These changes occur at protein level and not mRNA expression, since we have not observed changes in *Mapt* expression between VEH hippocampi and those treated with JZ1.40 (data not shown). Taken together, these results indicate that JZ1.40 can reduce the aggregation of p-TAU. To confirm these results, we performed co-immunofluorescence staining against TAU-total versus p-TAU (with AT8 antibody). The pictures show that in the non-injected side, there was almost no expression of either total hTAU or p-TAU in both experimental groups (Fig. 1E). Interestingly, in hTAU^{P301L} expressing neurons, we observed increased hTAU phosphorylation. Importantly, JZ1.40 significantly decreased hTAU phosphorylation. These results evidenced that JZ1.40 is able to reduce the hyperphosphorylation of TAU in a tauopathy mouse model.

3.3. JZ1.40 treatment ameliorates cognitive impairment induced by hTAU^{P301L}

To assess whether the treatment with the LRRK2 inhibitor, JZ1.40, could restore recognition memory alterations induced by TAU overexpression in the hippocampus, we performed the NOR test (Leger et al., 2013) just before the day of sacrifice. As a control group, we used WT mice from the same age, without hTAU^{P301L} overexpression or treatment. A control adeno-associated virus vector expressing green fluorescence protein did not elicit significant changes in inflammation or gliosis (Cuadrado et al., 2018; Lastres-Becker et al., 2014). WT mice overexpressing hTAU^{P301L} and treated with vehicle showed a significant decrease in DI compared to control animals. Interestingly, the treatment with JZ1.40 was able to restore DI to levels of control mice, indicating that the inhibition of LRRK2 activity could modulate the cognitive impairment induced by hTAU^{P301L} overexpression (Fig. 2A).

3.4. hTAU^{P301L} expression induces granular cell layer degeneration at the dentate gyrus which is prevented by JZ1.40 treatment

Within the hippocampus, the area of the dentate gyrus is thought to contribute to the formation of new episodic memories (Deng et al., 2010) and the spontaneous exploration of novel environments, among other functions. Therefore, we assessed if JZ1.40 treatment could modulate the neurodegeneration induced by hTAU^{P301L} overexpression. DAPI staining of the dentate gyrus area indicates that hTAU^{P301L} overexpression induces an upper granular cell layer loss in mice treated with vehicle (Fig. 2B and C) and a reduction in the below granular layer. Although the treatment with JZ1.40 was not able to protect from the hTAU^{P301L} induced neuronal loss of the upper layer, it can be observed that the lower granular layer was protected (neuronal thickening) (Fig. 2B and C).

As we have previously described in this model of tauopathy, hTAU^{P301L} expressing neurons do not express calbindin-D28K, a major calcium-binding and buffering protein, which has a critical role in preventing neuronal death as well as maintaining calcium homeostasis and synaptic plasticity (Castro-Sánchez et al., 2019; Cuadrado et al., 2018). Therefore, to determine if the protection observed in Fig. 2B and C correlated with calbindin-D28K expression levels, we performed a co-immunofluorescence analysis. At the dentate gyrus, hTAU^{P301L} overexpression reduces calbindin-D28K expression levels (Fig. 2D and E). On the other hand, mice treated with JZ1.40 exhibited higher calbindin-D28K expression in neurons at the lesioned side compared to vehicle mice (Fig. 2D and E), indicating that LRRK2 inhibition could protect against TAU-induced neurodegeneration at the granular cell layer of the dentate gyrus.

4. Discussion

Mutations in the LRRK2 gene are the most common cause of late-onset autosomal-dominant PD being the LRRK2-G2019S the more predominant associated mutation. Although Lewy bodies (composed of α-synuclein) are a main feature of PD, they are not

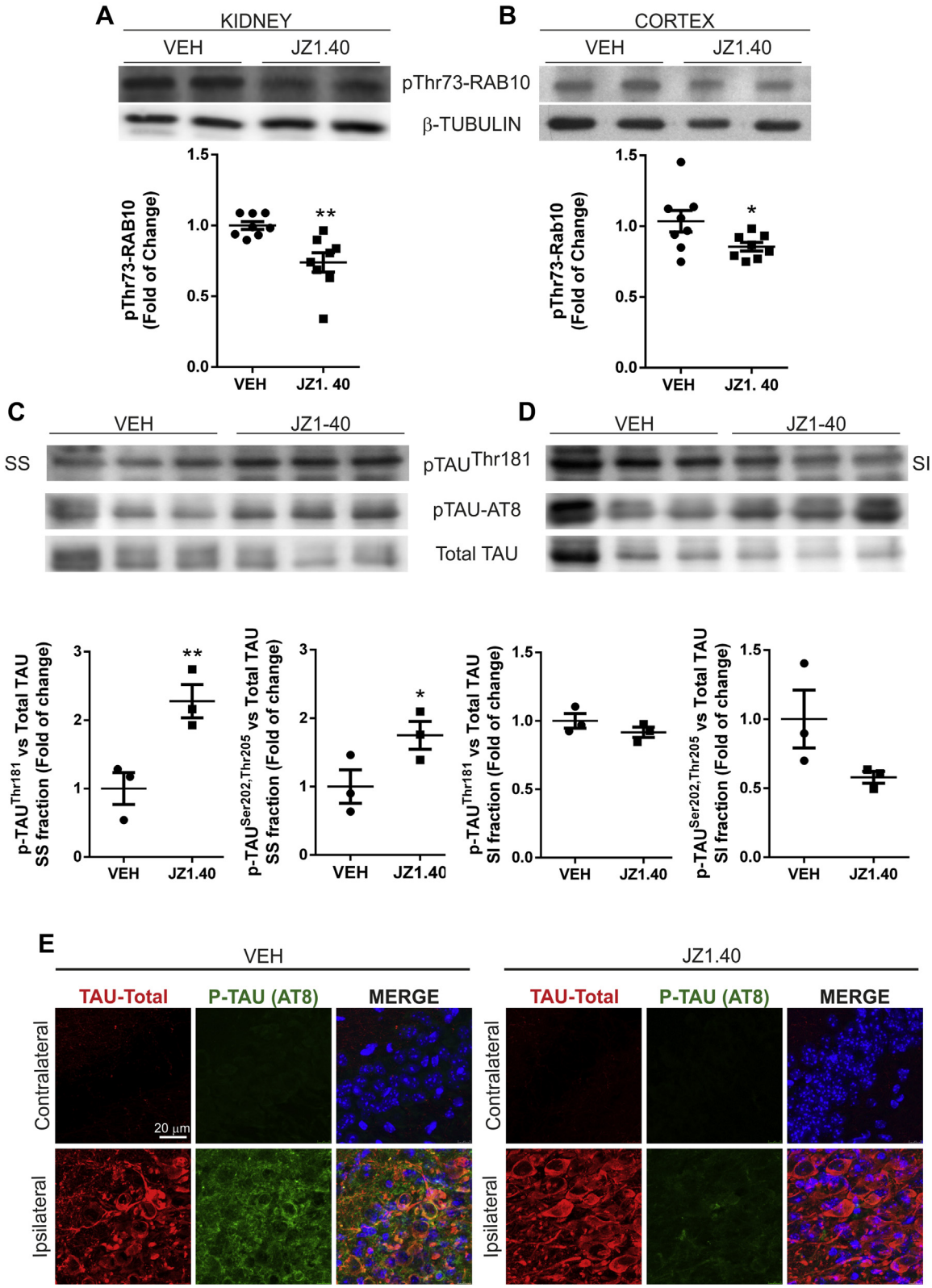

Fig. 1. Analysis of the target engagement of JZ1.40. (A, B) Immunoblot analysis in whole kidney and cortex lysates of protein levels of pThr73-RAB10 and β-TUBULIN as a loading control. Densitometric quantification of representative blots normalized for β-TUBULIN levels. Scatter blot indicates mean of n = 8 samples ± SEM. Asterisks denote significant differences with $*p < 0.05$ and $**p < 0.01$ comparing the indicated groups with a Student's *t*-test (F, DFn, Dfd: 6.229, 7,7; $t = 3.540$ and df = 14 for kidney; F, DFn, Dfd: 6.501, 7,7; $t = 2.204$ and df = 14 for cortex). JZ1.40 treatment increases p-TAU solubility. Ipsilateral hippocampal tissue obtained from our AAV-hTAU^{P301L} injected mice were separated into sarkosyl-soluble (SS) and insoluble (SI) fractions as described in "Materials and methods" section. The levels of p-TAU were analyzed in vehicle or JZ1.40 treated mice (n = 3 per experimental group) by immunoblotting using a monoclonal antibody to p-TAU Thr181 (C) or AT8 (Ser202/Thr205) (D), and their respective protein quantifications. Asterisks show significant differences with $*p < 0.05$ comparing each group according to a Student's *t*-test (SS p-TAU^{Thr181}: F, DFn, Dfd: 1.096, 2,2; $t = 3.803$ and df = 4; SS-AT8: F, DFn, Dfd: 1.422, 2,2; $t = 2.357$ and df = 4; SI p-TAU^{Thr181}: F, DFn, Dfd: 2.069, 2,2; $t = 1.265$ and df = 4; SI-AT8: F, DFn, Dfd: 24.09, 2,2; $t = 1.970$ and df = 4). (E) p-TAU levels decrease by JZ1.40 treatment in a mouse model of tauopathy. Double immunofluorescence staining of 30-μm thick sections of hippocampus from mice injected with AAV-hTAU^{P301L} (ipsilateral side) after 3 weeks treated with vehicle (left) or JZ1.40 (right). Red, anti-TAU total antibody; green, anti-p-TAU (AT8 antibody). Abbreviation: AAV, adeno-associated virus. (For interpretation of the references to color in this figure legend, the reader is referred to the Web version of this article.)

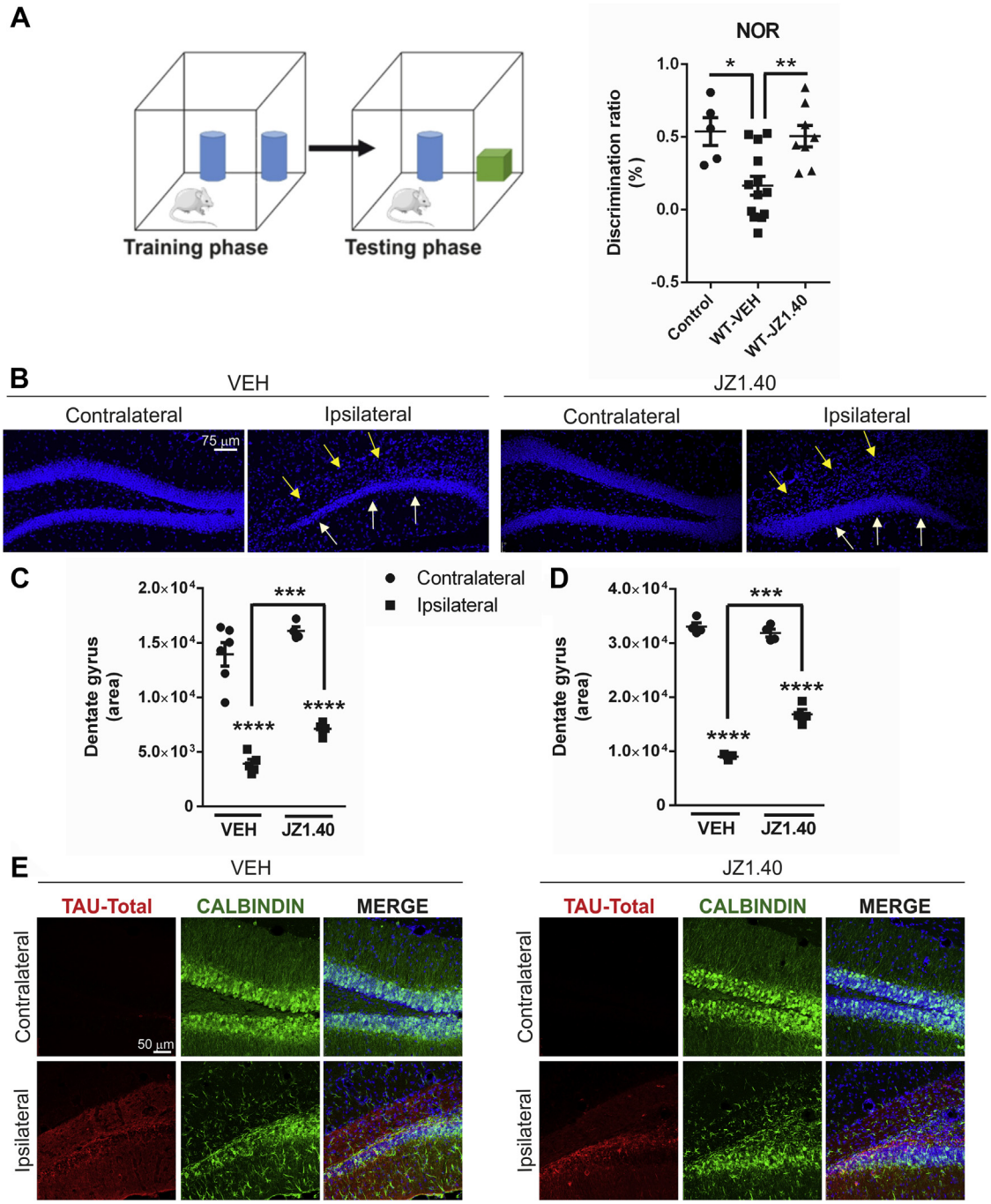

Fig. 2. Treatment with the LRRK2 inhibitor rescues the cognitive impairment induced by hTAU^{P301L} overexpression in mice. (A) Recognition memory was tested by novel object recognition test (NOR) at control mice, and mice overexpressing hTAU^{P301L} and treated with vehicle or LRRK2 inhibitor (JZ1.40), 2 days before the sacrifice (n = 14 VEH; n = 10 WT-JZ1.40; n = 7 WT-Control). Asterisks denote significant differences with $*p < 0.05$ and $**p < 0.01$, comparing each group with its respective control or the indicated groups, according to a one-way ANOVA test followed by Turkey's multiple comparisons test (F (DFn, DFd) $F(2,23) = 8.217$). JZ1.40 has a neuroprotective effect on the lower granular cell layer of the dentate gyrus. (B) DAPI immunofluorescence staining of 30-µm thick sections of the dentate gyrus of the hippocampus from AAV-hTAU^{P301L} mice treated with vehicle or JZ1.40. Yellow arrows indicate the disappeared upper layer of the dentate gyrus. White arrows show the remaining area of the dentate gyrus. (C) Quantification of the area stained with DAPI in the dentate gyrus from VEH and JZ1.40 treated mice injected with AAV-hTAU^{P301L}. Bars indicate the mean of n = 4–6 samples ± SEM. (D) Quantification of the area stained with calbindin-D28K in the dentate gyrus from VEH and JZ1.40 treated mice injected with AAV-hTAU^{P301L}. Bars indicate the mean of n = 4 samples ± SEM. (E) JZ1.40 treatment protects from dentate gyrus neuronal damage in the AAV-TAU^{P301L} mouse model. Double immunofluorescence staining of 30-µm thick sections of the dentate gyrus of hippocampus from mice injected with AAV-hTAU^{P301L} (ipsilateral side) after 3 weeks treated with vehicle (left) or JZ1.40 (right). Red, anti-TAU total antibody; green, anti-calbindin-D28K antibody. Asterisks denote significant differences with $***p < 0.001$ and $****p < 0.0001$ comparing the ipsilateral side with the contralateral side or the indicated groups, according to a one-way ANOVA followed by Bonferroni's multiple comparisons test (DAPI: Interaction $F(1,15) = 0.4685$, $p = 0.504$; Treatment $F(1,15) = 12.12$ $p = 0.0033$; Lesion $F(1,15) = 152.8$, $p < 0.0001$; calbindin-D28K: Interaction $F(1,11) = 36.56$, $p < 0.0001$; Treatment $F(1,11) = 19.95$ $p = 0.0010$; Lesion $F(1,11) = 689.0$ $p < 0.0001$). Abbreviation: AAV, adeno-associated virus. (For interpretation of the references to color in this figure legend, the reader is referred to the Web version of this article.)

present in all LRRK2-PD subjects. More recently, it has been hypothesized that TAU protein may act as a neuropathological substrate of Lewy bodies-negative LRRK2 PD (Henderson et al., 2019). It has been shown that TAU pathology is present in 100% carriers of LRRK2 mutations, indicating crosstalk between LRRK2 and TAU. Moreover, LRRK2 can influence the cytoskeleton of neurons reducing neurite outgrowth and cause hyperphosphorylation of TAU. Therefore, in this study we have analyzed, for the first time, the effects of an LRRK2 inhibitor on the in vivo modulation of TAU phosphorylation and its implication in the neurodegenerative process in an in vivo mouse model of tauopathy.

Our results show that the benzothiazole-based LRRK2 inhibitor JZ1.40 can cross the blood-brain barrier and inhibit LRRK2 in vivo showing a reduction of p-RAB10 both in kidneys and brain. Moreover, the LRRK2 inhibitor JZ1.40 modulates the phosphorylation state of TAU (Fig. 1C–E) in an AAV-hTAU^{P301L} overexpressing mouse model. Phenotypically, treated animals ameliorate cognitive impairment using the NOR test (Fig. 2A). This effect may be attributed to the modulation of TAU phosphorylation at epitope Thr181 (Fig. 1C), which is mediated by direct interaction with LRRK2 or at epitopes Ser202/Thr205 (Fig. 1D) associated to GSK-3β activation by direct LRRK2 activation (Kawakami et al., 2014). Moreover, JZ1.40 induces the solubilization of phosphorylated TAU (Fig. 1C and D), avoiding TAU aggregation. All these data suggest that JZ1.40 could be a potential therapeutic drug in the modulation of TAU phosphorylation state, through direct and indirect effects. Additionally, this LRRK2 inhibitor could be beneficial for the treatment of other pathologies, like PD.

Our data demonstrate that hTAU^{P301L} overexpression induces changes in calbindin-D28K levels at the dentate gyrus. Calbindin-D28K is a key player in spatial learning paradigms, motor coordination and neuronal survival, and some forms of synaptic plasticity (Westerink et al., 2012) and there is a marked reduction in calbindin-D28K expression in the brains of Alzheimer's disease patients and Alzheimer's disease mouse models (Kook et al., 2014). Our results agree with these observations since we see that hTAU^{P301L} overexpression significantly lowers calbindin-D28K levels (Fig. 2D and E) that correlate with impaired NOR (Fig. 2A). Furthermore, treatment with JZ1.40 partially restores calbindin-D28K levels avoiding massive degeneration of the neurons of the dentate gyrus (Fig. 2D and E), which correlates with an improvement in the performance of NOR.

Altogether, these data show not only that JZ1.40 reaches the brain and modulates TAU phosphorylation at the epitopes modified by LRRK2, but also plays a significant role in neuroprotection in vivo which is translated to cognition enhancement.

5. Conclusions

Our results indicate that LRRK2 inhibitors and, specifically, the benzothiazole JZ1.40 could be the first step to cover a future therapy against tauopathies, as we have seen beneficial effects in our AAV-TAU^{P301L} model, although further studies on the mechanism of action and side effects need to be evaluated.

Disclosure statement

No conflicts of interest have been reported by any of the authors involved in the publication of this study.

Acknowledgements

This work was supported by MINECO (Competitiveness Grants SAF2016-76520-R to ILB, SAF2016-76693-R to AM, and RTI2018-095793-B-I00 to MGL), MECD (FPU grant FPU13-003262 to JZD), SCS is beneficiary of the call for predoctoral contracts for the training of research personnel 2018 (FPI-UAM) and Fundación Tatiana Pérez de Guzmán el Bueno to EL.

I.L.B. and A.M. contributed to the conception and design of the study. J.Z., C.G., and A.M. generated the compound JZ1.40, an LRRK2 inhibitor. E.L., S.C.S., and M.G.L. were implicated in the novel recognition analysis. S.C.S. and I.L.B. helped in acquisition and analysis of data. I.L.B. and A.M. contributed to drafting a significant portion of the manuscript and figures.

Study design: The study was not pre-registered.

Appendix A. Supplementary data

Supplementary data to this article can be found online at https://doi.org/10.1016/j.neurobiolaging.2020.09.006.

References

Bailey, R.M., Covy, J.P., Melrose, H.L., Rousseau, L., Watkinson, R., Knight, J., Miles, S., Farrer, M.J., Dickson, D.W., Giasson, B.I., Lewis, J., 2013. LRRK2 phosphorylates novel tau epitopes and promotes tauopathy. Acta Neuropathol. 126, 809–827.

Castro-Sánchez, S., García-Yagüe, Á.J., Kügler, S., Lastres-Becker, I., 2019. CX3CR1-deficient microglia shows impaired signaling of the transcription factor NRF2: implications in tauopathies. Redox Biol. 101118.

Castro-Sanchez, S., Garcia-Yague, A.J., Lopez-Royo, T., Casarejos, M., Lanciego, J.L., Lastres-Becker, I., 2018. Cx3cr1-deficiency exacerbates alpha-synuclein-A53T induced neuroinflammation and neurodegeneration in a mouse model of Parkinson's disease. Glia.

Cuadrado, A., Kugler, S., Lastres-Becker, I., 2018. Pharmacological targeting of GSK-3 and NRF2 provides neuroprotection in a preclinical model of tauopathy. Redox Biol. 14, 522–534.

Curtis, M.J., Alexander, S., Cirino, G., Docherty, J.R., George, C.H., Giembycz, M.A., Hoyer, D., Insel, P.A., Izzo, A.A., Ji, Y., MacEwan, D.J., Sobey, C.G., Stanford, S.C., Teixeira, M.M., Wonnacott, S., Ahluwalia, A., 2018. Experimental design and analysis and their reporting II: updated and simplified guidance for authors and peer reviewers. Br. J. Pharmacol. 175, 987–993.

Deng, W., Aimone, J.B., Gage, F.H., 2010. New neurons and new memories: how does adult hippocampal neurogenesis affect learning and memory? Nat. Rev. Neurosci. 11, 339–350.

Eyers, P.A., 2016. 'Up with the LRRK': a phosphorylated Rab10 assay for evaluation of LRRK2 activity and inhibitor engagement. Biochem. J. 473, 2757–2762.

Hamm, M., Bailey, R., Shaw, G., Yen, S.H., Lewis, J., Giasson, B.I., 2015. Physiologically relevant factors influence tau phosphorylation by leucine-rich repeat kinase 2. J. Neurosci. Res. 93, 1567–1580.

Henderson, M.X., Sengupta, M., Trojanowski, J.Q., Lee, V.M.Y., 2019. Alzheimer's disease tau is a prominent pathology in LRRK2 Parkinson's disease. Acta Neuropathol. Commun. 7, 183.

Ito, G., Katsemonova, K., Tonelli, F., Lis, P., Baptista, M.A., Shpiro, N., Duddy, G., Wilson, S., Ho, P.W., Ho, S.L., Reith, A.D., Alessi, D.R., 2016. Phos-tag analysis of Rab10 phosphorylation by LRRK2: a powerful assay for assessing kinase function and inhibitors. Biochem. J. 473, 2671–2685.

Kawakami, F., Shimada, N., Ohta, E., Kagiya, G., Kawashima, R., Maekawa, T., Maruyama, H., Ichikawa, T., 2014. Leucine-rich repeat kinase 2 regulates tau phosphorylation through direct activation of glycogen synthase kinase-3beta. FEBS J. 281, 3–13.

Kook, S.Y., Jeong, H., Kang, M.J., Park, R., Shin, H.J., Han, S.H., Son, S.M., Song, H., Baik, S.H., Moon, M., Yi, E.C., Hwang, D., Mook-Jung, I., 2014. Crucial role of calbindin-D28k in the pathogenesis of Alzheimer's disease mouse model. Cell Death Differ. 21, 1575–1587.

Lastres-Becker, I., Innamorato, N.G., Jaworski, T., Rabano, A., Kugler, S., Van Leuven, F., Cuadrado, A., 2014. Fractalkine activates NRF2/NFE2L2 and heme oxygenase 1 to restrain tauopathy-induced microgliosis. Brain 137 (Pt 1), 78–91.

Leger, M., Quiedeville, A., Bouet, V., Haelewyn, B., Boulouard, M., Schumann-Bard, P., Freret, T., 2013. Object recognition test in mice. Nat. Protoc. 8, 2531–2537.

Ren, C., Ding, Y., Wei, S., Guan, L., Zhang, C., Ji, Y., Wang, F., Yin, S., Yin, P., 2019. G2019S variation in LRRK2: an ideal model for the study of Parkinson's disease? Front. Hum. Neurosci. 13, 306.

Ren, Y., Sahara, N., 2013. Characteristics of tau oligomers. Front. Neurol. 4, 102.

Ruffmann, C., Giaccone, G., Canesi, M., Bramerio, M., Goldwurm, S., Gambacorta, M., Rossi, G., Tagliavini, F., Pezzoli, G., 2012. Atypical tauopathy in a patient with LRRK2-G2019S mutation and tremor-dominant Parkinsonism. Neuropathol. Appl. Neurobiol. 38, 382–386.

Salado, I.G., Zaldivar-Diez, J., Sebastian-Perez, V., Li, L., Geiger, L., Gonzalez, S., Campillo, N.E., Gil, C., Morales, A.V., Perez, D.I., Martinez, A., 2017. Leucine rich repeat kinase 2 (LRRK2) inhibitors based on indolinone scaffold: potential pro-neurogenic agents. Eur. J. Med. Chem. 138, 328–342.

Sanchez-Contreras, M., Heckman, M.G., Tacik, P., Diehl, N., Brown, P.H., Soto-Ortolaza, A.I., Christopher, E.A., Walton, R.L., Ross, O.A., Golbe, L.I., Graff-Radford, N., Wszolek, Z.K., Dickson, D.W., Rademakers, R., 2017. Study of LRRK2

variation in tauopathy: progressive supranuclear palsy and corticobasal degeneration. Mov. Disord. 32, 115–123.
Vilas, D., Sharp, M., Gelpi, E., Genis, D., Marder, K.S., Cortes, E., Vonsattel, J.P., Tolosa, E., Alcalay, R.N., 2018. Clinical and neuropathological features of progressive supranuclear palsy in Leucine rich repeat kinase (LRRK2) G2019S mutation carriers. Mov. Disord. 33, 335–338.
Wallings, R., Manzoni, C., Bandopadhyay, R., 2015. Cellular processes associated with LRRK2 function and dysfunction. FEBS J. 282, 2806–2826.
Wang, Y., Mandelkow, E., 2016. Tau in physiology and pathology. Nat. Rev. Neurosci. 17, 5–21.
Westerink, R.H.S., Beekwilder, J.P., Wadman, W.J., 2012. Differential alterations of synaptic plasticity in dentate gyrus and CA1 hippocampal area of Calbindin-D28K knockout mice. Brain Res. 1450, 1–10.
Zaldivar-Diez, J., Li, L., Garcia, A.M., Zhao, W.N., Medina-Menendez, C., Haggarty, S.J., Gil, C., Morales, A.V., Martinez, A., 2019. Benzothiazole-based LRRK2 inhibitors as Wnt enhancers and promoters of oligodendrocytic fate. J. Med. Chem.